

Single production of vectorlike quarks with charge 5/3 at the 14 TeV LHC

Yao-Bei Liu*, Bo Hu, Chao-Zheng Li

Henan Institute of Science and Technology, Xinxiang 453003, P.R. China

Abstract

Vector-like quarks arise in various new physics scenarios beyond the Standard Model (SM). In a framework of the SM simply extended by an $SU(2)$ doublet (X, T) including a vector-like quark X (VLQ- X), with electric charge $|Q_X| = 5/3$, we investigate the single production of the VLQ- X induced by the couplings between the VLQ- X with the first and the third generation quarks at the Large Hadron Collider (LHC) Run-III and High-Luminosity LHC (HL-LHC) operating at $\sqrt{s} = 14$ TeV. The signal is searched in events including same-sign dileptons (electrons or muons), one b -tagged jet and missing energy, where the X quark is assumed to decay into a top quark and a W boson, both decaying leptonically. After a rapid simulation of signal and background events, the 95% CL exclusion limits and the 5σ discovery reach are respectively obtained at the 14 TeV LHC with an integrated luminosity of 300 and 3000 fb^{-1} , respectively.

* E-mail: liuyaobei@hist.edu.cn

I. INTRODUCTION

To promote a potential solution to the hierarchy problem [1], new heavy vector-like quarks (VLQs) are generally predicted in many new physics models beyond the SM (BSM), such as little Higgs [2–4], composite Higgs [5, 6], and other extended models [7–10]. Such VLQs are color triplets and their left-handed and right-handed components transform in the same way under the $SU(2) \times U(1)$ gauge group. In the renormalizable extensions of the SM that include VLQs, the canonical representation of VLQs constitutes one of seven multiplets VLQs, including two singlet $[T, B]$, three doublets $[(X, T), (T, B) \text{ or } (B, Y)]$, and two triplets $[(X, T, B) \text{ or } (T, B, Y)]$. The T and B are often referred as the top and bottom partner, and the Y and X quarks have exotic electric charge $-4e/3$ and $5e/3$, respectively. Here we focus on the vector-like X -quark (VLQ- X) which always occurs as part of an $SU(2)_L \times SU(2)_R$ bi-doublet in models that preserve custodial symmetry [14, 15] and in models where VLQ multiplets are added via renormalisable couplings [16–19]. Such new particles could also provide rich phenomenology at the current and future high-energy colliders [20–27].

The signal of VLQ- X has been widely searched by the ATLAS and CMS collaborations at the Large Hadron Collider (LHC) [28–34]. The searches are focusing mainly on the pair-production modes via its QCD interactions, since the cross-section for which depends only on the VLQ mass. For instance, CMS Collaboration used an integrated luminosity 35.9 fb^{-1} of data and provided the lower mass bounds about 1.30 (1.33) TeV at 95% confidence level (C.L.), for the case of left (right)-handed couplings to W bosons in a combination of the same-sign dileptons and single-lepton final states [35]. Recently, the search was carried out on 139 fb^{-1} of proton-proton collision data at $\sqrt{s} = 13 \text{ TeV}$ with the ATLAS detector between 2015 and 2018 runs [36]. This search excluded the presence of a $X_{5/3}$ with mass up to 1.46 TeV for (X,T) doublets for $Br(X \rightarrow tW) = 1$. Besides, such VLQ- X can also be singly produced at the LHC via its EW coupling, which depends on the coupling strength [37–39]. Considering the final state including one muon or electron, the existence of VLQ- X with left-handed couplings and a relative width of 10, 20, and 30% can be excluded for masses below 0.92, 1.3, and 1.45 TeV respectively at the $\sqrt{s} = 13 \text{ TeV}$ LHC with 35.9 fb^{-1} luminosity by the CMS Collaboration [40].

However, most of the studies are based on the assumption that the $X_{5/3}$ quarks only decay into the tW final state. Note that VLQs that mixing to the first- and second-generation SM

quarks is not completely excluded [17]. The ATLAS Collaboration has provided the lower mass bounds about 350 GeV at 95% CL via the pair production with both $X_{5/3}$ decaying into Wq , with q being any light quark [41]. In Ref. [42], corresponding to an integrated luminosity of 4.64 fb^{-1} , the single production of heavy quarks decaying only to light generations is studied: the quoted bound for $X_{5/3}$ is $m_X > 1420 \text{ GeV}$ for the fixed coupling $\tilde{\kappa}_{qQ} = 1$.

The upgrade of the LHC to the high-luminosity phase (HL-LHC) [43] at center-of-mass energy of 14 TeV and integrated luminosity of 3000 fb^{-1} will extend the sensitivity and perspectives to discover possible NP signals. Due to the exotic charge, its main distinctive decay mode is $X \rightarrow W^+ t \rightarrow W^+ W^+ b$ [44, 45], which can give rise to the final states including same-sign two leptons (SS2L) via the W leptonic decays. In comparison with the existing searches for other channels, the SS2L channel has the great advantage that most QCD backgrounds are gone, such as done in Refs. [46–52]. Considering $X_{5/3}$ pair production and looking for a SS2L channel, the bounds on the $X_{5/3}$ mass obtained from ATLAS (CMS) is $M_X > 670$ (675) GeV with a sample corresponding to an integrated luminosity of 4.7 (5) fb^{-1} [53, 54]. Very recently, the authors of Refs. [55, 56] investigated the prospect of discovering the doublet right-handed $X_{5/3}$ via the single production channel $pp \rightarrow X \bar{t} j$ at the high energy pp colliders. Note however that all these searches focus on the assumption that $X_{5/3}$ mixing only to third generation SM quarks. Considering the constraints from flavor physics [57, 59], the VLQs can mix in a sizable way with the first generation quark, which could have a severe impact on their single production (via EW interactions) at the LHC due to the presence of valence quarks in the initial state [60, 61]. In this work, we study the single production of the VLQ- X at the HL-LHC in a simplified scenario where the $X_{5/3}$ quarks could mixing with both the the first-generation and the third-generation SM quarks, as shown in Fig. 1, and then analyze the SS2L final state via $X \rightarrow t(\rightarrow bW^+)W^+$ decay channel followed by the W leptonic decays mode.

The paper is arranged as follows. In Sec. II, we consider an effective model framework including the $X_{5/3}$ and calculate its single production cross sections at the 14 TeV LHC involving the mixing with both the first and third generate quarks. In Sec. III, we discuss its observability via the decay mode $X \rightarrow t(\rightarrow bW^+)W^+ \rightarrow \ell^+ \ell^+ b + \cancel{E}_T$ at the HL-LHC. Finally, conclusions are presented in Sec. IV.

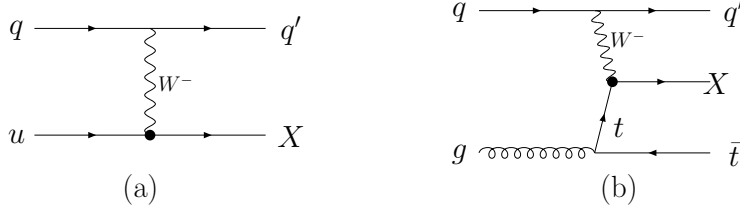


FIG. 1: Representative Feynman diagrams for the single production processes at the LHC via couplings of the X to (a) first generation quarks and (b) third generation quarks.

II. VLQ- X IN A SIMPLIFIED MODEL

A. An effective Lagrangian for doublet VLQ- X

We focus on a specific simple model containing a vector-like quark which is an $SU(2)$ doublet with hypercharge $7/6$. Such a doublet also contains a top partner T due to its mixing with SM up-type quarks (see for example [57] and references therein). In the weak eigenstate basis of the (X, T) doublet, the masses of the new heavy quarks are given by [16, 17],

$$\mathcal{L}_{mass} = -(t_L^0 \ T_L^0) \begin{pmatrix} y_t \frac{v}{\sqrt{2}} & 0 \\ y_i \frac{v}{\sqrt{2}} & M_0 \end{pmatrix} \begin{pmatrix} t_R^0 \\ T_R^0 \end{pmatrix} + h.c., \quad (1)$$

where $t_{L,R}^0$ is the left (right)-handed top quark weak eigenstates, $T_{L,R}^0$ is the left (right)-handed vector-like top quark weak eigenstates. y_i are the new Yukawa couplings, $v \sim 246$ GeV is the Higgs vacuum expectation value (VEV), M_0 is the vector-like quark mass (also equal to the mass of $X_{5/3}$, $M_X = M_0$).

When the T quark only mixes with the top quark, the relationship between the weak eigenstates and the mass eigenstates $t_{L,R}$, $T_{L,R}$ can be parameterized by two 2×2 unitary matrices,

$$\begin{pmatrix} t_{L,R} \\ T_{L,R} \end{pmatrix} = \begin{pmatrix} \cos \theta_{L,R} & -\sin \theta_{L,R} \\ \sin \theta_{L,R} & \cos \theta_{L,R} \end{pmatrix} \begin{pmatrix} t_{L,R}^0 \\ T_{L,R}^0 \end{pmatrix}, \quad (2)$$

where $\theta_{L,R}$ denotes the left (right) mixing angle. Then, the mass matrix can be diagonalized as

$$\begin{pmatrix} \cos \theta_L & -\sin \theta_L \\ \sin \theta_L & \cos \theta_L \end{pmatrix} \begin{pmatrix} y_t \frac{v}{\sqrt{2}} & 0 \\ y_i \frac{v}{\sqrt{2}} & M_0 \end{pmatrix} \begin{pmatrix} \cos \theta_R & \sin \theta_R \\ -\sin \theta_R & \cos \theta_R \end{pmatrix} = \begin{pmatrix} m_t & 0 \\ 0 & m_T \end{pmatrix} \quad (3)$$

Thus we can obtain that

$$\tan \theta_L = \frac{m_t}{m_T} \tan \theta_R, \quad (4)$$

and

$$M_X^2 = M_0^2 = m_T^2 \cos^2 \theta_R + m_t^2 \sin^2 \theta_R. \quad (5)$$

Note that the mixing angle for left-handed components θ_L is typically smaller than the right-handed one θ_R , being suppressed by the mass of the top over the heavy mass M_0 (which is typically larger). This property is still valid in the case of mixing with three flavours, with the left-handed mixing terms proportional to the light quark masses, while the right-handed ones are proportional to the Yukawa masses [62]. Therefore, the terms in the Lagrangian with regard to $\sin \theta_L$ can be safely neglected.

Under the assumption that the VLQ- X couples only to the first- and third-generation quarks, an effective Lagrangian that parametrizes the $X_{5/3}$ quark couplings to quarks and electroweak bosons is given by [63]¹

$$\mathcal{L}_X = \frac{g^*}{2} \left\{ \sqrt{\frac{R_L}{1+R_L}} \frac{g}{\sqrt{2}} [\bar{X}_R W_\mu^+ \gamma^\mu u_R] + \sqrt{\frac{1}{1+R_L}} \frac{g}{\sqrt{2}} [\bar{X}_R W_\mu^+ \gamma^\mu t_R] \right\} + h.c., \quad (6)$$

where g is the $SU(2)_L$ gauge coupling constant, g^* indicates the $X_{5/3}$ coupling strength to SM quarks in units of standard couplings, and R_L is generation mixing coupling, which controls the share of the $X_{5/3}$ coupling between first- and third- generation quarks. In the extreme case, $R_L = 0$ and $R_L \rightarrow \infty$, respectively, correspond to coupling to third generation quarks and first generation of quarks only.

The mixing of VLQs simultaneously with more than one SM family is strongly constrained by the flavor physics and the oblique parameters [62–64]. The strong limit for the up quark mixing come from Atomic Parity Violation (APV) experiments: $V_R^{41} < 7.8 \times 10^{-2}$ [57]. The recent bound on the coupling parameter g^* comes from the oblique parameters S , T and U , i.e., $\sin \theta_R < 0.2$ for the (X, T) doublet [58]. These bounds convert to $\frac{g^*}{2} \sqrt{\frac{R_L}{1+R_L}} = V_R^{41} <$

¹ Details are provided on the URL feynrules.irmp.ucl.ac.be/wiki/VLQ_xtdoubletvl.

7.8×10^{-2} and $\frac{g^*}{2} \sqrt{\frac{1}{1+R_L}} = \sin \theta_R < 0.2$ for our parameters, respectively. Here we take only a phenomenologically guided limit and take a conservative value: $g^* \leq 0.5$ and $0 \leq R_L \leq 1$.

B. Decay and production cross section

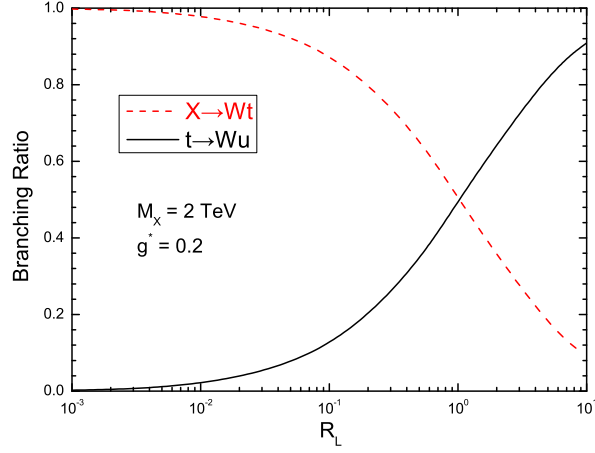


FIG. 2: The branching ratio as a function of R_L for $g^* = 0.2$ and $M_X = 2.0$ TeV.

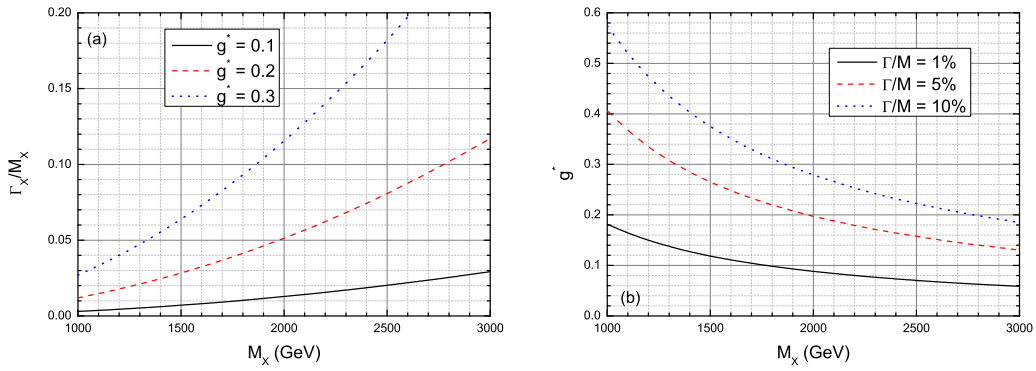


FIG. 3: (a) The width-over-mass ratio Γ_X/M_X as a function of M_X for three typical coupling strength $g^* = 0.1, 0.2$ and 0.3 . (b) The value of g^* as a function of M_X for different width-over-mass ratio $\Gamma_X/M_X = 1\%, 5\%$ and 10% .

Due to its charge, the VLQ- X can decay only to Wt and Wu therefore $BR(X \rightarrow Wt) + BR(X \rightarrow Wu) = 100\%$, as shown in Fig. 2. Note that, when R_L up to 1.0, the decay rate of $X_{5/3}$ to the first-generation quark reaches to the same value of $X_{5/3}$ to the third-generation quark decay. The decay width depends on the coupling parameter g^* and its mass M_X . For a fixed VLQ- X mass, the total width Γ_X is always proportional to $(g^*)^2$, as shown in Fig. 3(a). Therefore, the coupling strength g^* can also be fixed to obtain a specific width-over-mass ratio Γ_X/M_X , as shown in Fig. 3(b). One can see that, for the scenario $\Gamma_X/M_X = 10\%$, g^* is approximately smaller than 0.2 in the whole range of explored masses. It has been pointed out in [65] that the Breit-Wigner (BW) form of a propagator may be appropriate for narrow resonances where the width to mass ratio is smaller than 10%. Thus the VLQ- X can be assumed with narrow decay widths and the production and decay can be factorised under the narrow-width approximation (NWA) case ².

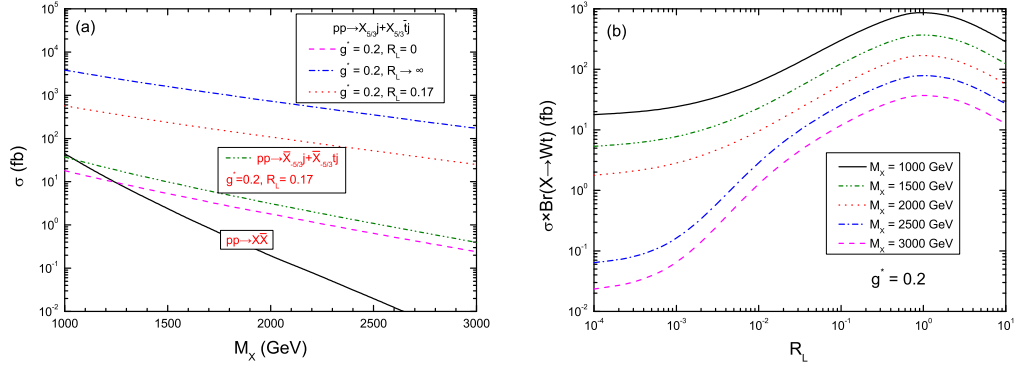


FIG. 4: (a) Cross sections of $X_{5/3}$ as a function of the mass M_X for single and pair production processes at the 14 TeV LHC. (b) Production cross section of $\sigma \times Br(X \rightarrow tW)$ as a function of R_L for $g^* = 0.2$ and five typical mass M_X at the 14 TeV LHC.

The VLQ- X can be both single and pair produced. The cross sections of single VLQ- X production versus its mass at the 14 TeV LHC has been presented in Fig. 4(a) with different coupling parameters. The leading-order (LO) cross sections are obtained using MadGraph5-aMC@NLO [66] with NNPDF23L01 parton distribution functions (PDFs) [67] taking the de-

² See Refs. [37–39] for large-width effects in vector-like quark production.

fault renormalization and factorization scales. One can note that pair production, is only dominant at low masses of the VLQ- X but decreases faster than single production when the mass of the $X_{5/3}$ quark increases. This is due to the phase space suppression and the decrease of the parton distribution functions with the centre of mass energy of the parton-level collision. However, single heavy quark production has the advantage of less phase-space suppression and longitudinal gauge boson enhancement of order m_X^2/m_W^2 at higher energies compared to pair production. With the fixed parameters $g^* = 0.2$ and $R_L = 0.17$, the cross section can reach about 236 (108) fb for $M_X = 1.5$ (2) TeV. We also plot the cross section for the process $pp \rightarrow \bar{X}j + \bar{X}tj$ for the same fixed coupling parameters. One can see that the production cross section of $pp \rightarrow Xj + X\bar{t}j$ is much larger than that for the conjugate process due to the difference in the PDFs of valence and sea quarks in the initial states.

In Fig. 4(b), we also show the dependence of the cross sections $\sigma \times Br(X \rightarrow tW)$ on the mixing parameter R_L . We generate five benchmark points varying the $X_{5/3}$ quark mass in steps of 500 GeV in the range [1000; 3000] GeV with $g^* = 0.2$. One can see that (i) in the range of $R_L < 1$, the production cross section increases largely with the increase of R_L . (ii) For $R_L > 1$, the production cross section will become small with the increase of R_L . This effect is mainly due to the increased admixture of valence quarks in production, mitigated by a reduced $X \rightarrow tW$ branching ratio with increasing R_L . The cross section will reach a maximum for $R_L \simeq 1$, which corresponds to 50% – 50% mixing.

III. EVENT GENERATION AND DISCOVERY POTENTIALITY

In this section we analyze the HL-LHC observation potential by performing a Monte Carlo (MC) simulation of the signal plus background events and explore the sensitivity to the VLQ- X through the process

$$\begin{aligned} pp \rightarrow X(\rightarrow tW^+)j &\rightarrow t(\rightarrow bW^+ \rightarrow b\ell^+\nu_\ell)W^+(\rightarrow \ell^+\nu_\ell)j, \\ pp \rightarrow X(\rightarrow tW^+)\bar{t}j &\rightarrow t(\rightarrow bW^+ \rightarrow b\ell^+\nu_\ell)W^+(\rightarrow \ell^+\nu_\ell)\bar{t}j, \end{aligned} \quad (7)$$

where $\ell = e, \mu$.

In this analysis, the final states with SSL (muon or electron), one b -tagged jet, and missing transverse energy \cancel{E}_T are studied. Note that we do not consider the reconstruction or selection for the associated anti-top quark as well as the leptons or jets originating from its decay, due

to their much lower transverse momenta p_T . The dominant SM backgrounds come from the SM processes $t\bar{t}W^+$, W^+W^+ +jets and the nonprompt leptons (mainly from events with jets of heavy flavor, such as $t\bar{t}$). Other processes, such as the $t\bar{t}Z$, triboson events, and ZW^\pm +jets are not included in the analysis owing to the negligible cross sections after the cuts. To account for contributions from higher-order QCD corrections, the cross sections of dominant backgrounds at LO are adjusted to NLO or next-NLO (NNLO) order by means of K factors, which are listed in table I.

TABLE I: K -factors of the leading SM background processes for our analysis.

Process	W^+W^+jj	$t\bar{t}W^+$	$t\bar{t}$
K -factor	1.04 [68, 69]	1.22 [70]	1.6 [71]

Signal and background events are generated at LO using MadGraph5-aMC@NLO. As a reference point, we set a benchmark value of $g^* = 0.2$ and $R_L = 0.17$. Analogously, our benchmark points in the mass axis read $M_X = 1500, 1800$ and 2000 GeV. To perform the parton shower and fast detector simulations, we transmit the parton-level events to Pythia 8 [72] for parton showering and hadronization, and Delphes 3.4.2 [73] for detector simulation by using the standard HL-LHC detector parameterization shipped with the program. Finally, event analysis is performed by using MadAnalysis5 [74].

To identify objects, the basic cuts at parton level for the signals and SM backgrounds are chosen as follows:

$$p_T^{\ell/j} > 30 \text{ GeV}, \quad |\eta_\ell| < 2.5, \quad |\eta_j| < 5, \quad \Delta R_{ij} > 0.4, \quad (8)$$

where $\Delta R = \sqrt{\Delta\Phi^2 + \Delta\eta^2}$ is the separation in the rapidity-azimuth plane and $p_T^{\ell/j}$ and $|\eta_{\ell/j}|$ are the transverse momentum and pseudorapidity of the leptons and jets, respectively.

In Fig. 5, we plot some differential distributions for signals and SM backgrounds at the LHC, such as the transverse momentum distributions of the leading and subleading leptons ($p_T^{\ell_{1,2}}$), the separations $\Delta R_{\ell_1, \ell_2}$ and $\Delta R_{\ell_2, b}$, the rapidity of the forward jet and the transverse mass³ distribution for VLQ- X $M_T^{b\ell_1\ell_2}$. Owing to the larger mass of VLQ- X , the decay products are

³ The definition of the transverse mass of the system can be seen from Ref. [75].

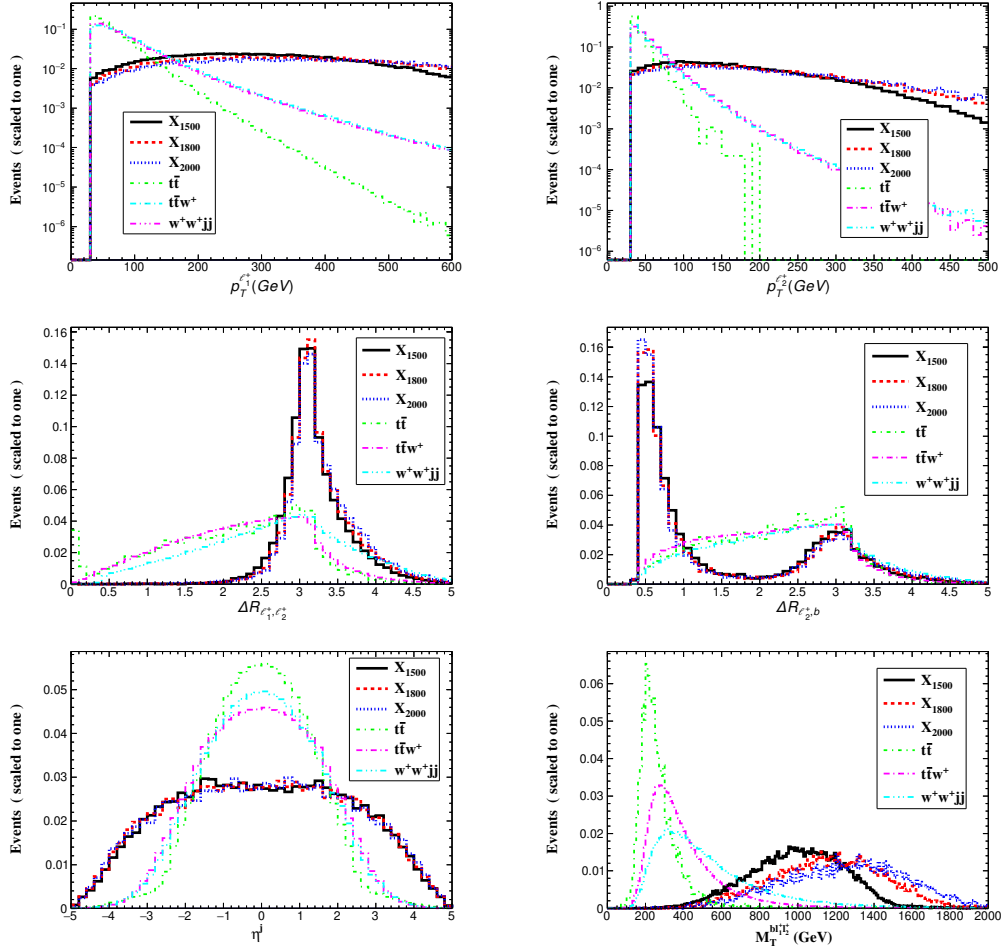


FIG. 5: Normalized distributions for the signals (with $M_X = 1500, 1800$ and 2000 GeV) and SM backgrounds.

highly boosted, and thus the p_T^ℓ peaks of the signals are larger than those of the SM backgrounds. Based on these kinematical distributions, we apply the following kinematic cuts to the events to distinguish the signal from the SM backgrounds.

- Cut 1: Exactly two same-sign isolated leptons [$N(\ell^+) = 2$] and the transverse momenta of the leading and subleading leptons are required $p_T^{\ell_{1,2}} > 120$ (60) GeV, the distance between two leptons lies in $\Delta R_{\ell_1, \ell_2} > 2.5$.
- Cut 2: At least one b -tagged jet. Besides, the distance between the subleading leptons with the b -tagged jet is required $\Delta R_{\ell_2, b} < 1$.

- Cut 3: Since the jet from splitting of a valence quark with one W emission always has a strong forward nature, the light untagged jet is required to have $|\eta_j| > 2$.
- Cut 4: The transverse mass of final system is required to have $M_T^{b\ell_1\ell_2} > 600$ GeV.

TABLE II: Cut flow of the cross sections (in fb) for the signals and SM backgrounds at the 14 TeV LHC and three typical VLQ- X masses.

Cuts	Signals			Backgrounds		
	1500 GeV	1800 GeV	2000 GeV	$t\bar{t}$	$t\bar{t}W^+$	W^+W^+jj
Basic	6.18	3.88	2.86	18741	11.1	2.73
Cut 1	2.44	1.38	0.94	0.1	0.32	0.11
Cut 2	0.78	0.44	0.28	0.01	0.06	8×10^{-4}
Cut 3	0.37	0.20	0.13	0.0022	0.009	1×10^{-4}
Cut 4	0.36	0.197	0.125	0.0011	0.0046	7.7×10^{-5}
Efficiency	5.8%	5.1%	4.4%	5.9×10^{-8}	4.2×10^{-4}	2.8×10^{-5}

We present the cross sections of three typical signal ($M_X = 1500, 1800, 2000$ GeV) and the relevant backgrounds after imposing the above mentioned cuts in Table II. The signal efficiencies for $M_X = 1500$ and 2000 GeV are 5.8% and 4.4%, respectively. Notably, all background processes are suppressed very significantly at the end of the cut flow, and the dominant SM background comes from the $t\bar{t}W^+$ process, with a cross section of about 0.005 fb.

We use the median significance to estimate the expected discovery and exclusion significance [76]

$$\mathcal{Z}_{\text{disc}} = \sqrt{2 \left[(s+b) \ln \left(\frac{(s+b)(1+\delta^2 b)}{b+\delta^2 b(s+b)} \right) - \frac{1}{\delta^2} \ln \left(1 + \delta^2 \frac{s}{1+\delta^2 b} \right) \right]}$$

$$\mathcal{Z}_{\text{excl}} = \sqrt{2 \left[s - b \ln \left(\frac{b+s+x}{2b} \right) - \frac{1}{\delta^2} \ln \left(\frac{b-s+x}{2b} \right) \right] - (b+s-x) \left(1 + \frac{1}{\delta^2 b} \right)}, \quad (9)$$

with

$$x = \sqrt{(s+b)^2 - 4\delta^2 s b^2 / (1 + \delta^2 b)}, \quad (10)$$

where s and b denote the event numbers after the above cuts for the signal and background, respectively. The integrated luminosity at the 14 TeV LHC is set at 300 and 3000 fb $^{-1}$, which

corresponds to the maximum achievable integrated luminosity during LHC Run-III and HL-LHC, respectively. δ denotes the percentage systematic error on the SM background estimate. In the limit case ($\delta \rightarrow 0$), these expressions can be simplified as

$$\begin{aligned} \mathcal{Z}_{\text{disc}} &= \sqrt{2[(s+b)\ln(1+s/b) - s]}, \\ \mathcal{Z}_{\text{excl}} &= \sqrt{2[s - b\ln(1+s/b)]}, \end{aligned} \quad (11)$$

as already used in many of the phenomenological studies.

In Fig. 6, we plot the excluded the 95% CL exclusion limit and 5σ discovery reaches in the plane of $g^* - M_X$ at the 14 TeV LHC with an integrated luminosity of 300 fb^{-1} and 3000 fb^{-1} respectively for three different systematic uncertainty cases: no systematics ($\delta=0$), a mild systematic of $\delta=10\%$, and an possible systematic of $\delta=20\%$. One can see that with a possible uncertainty of 20%, sensitivities are slightly weaker than those with a mild systematic uncertainty of 10% and no systematics of $\delta=0$. In the presence of 10% systematic uncertainty and $R_L = 0$, the discovered (with 5σ level) regions are $g^* \in [0.21, 0.4]$ ($[0.1, 0.4]$) and $M_X \in [1000, 1550]$ ($[1000, 2000]$) GeV at the 14 TeV LHC with an integrated luminosity of 300 (3000) fb^{-1} . Out of a discovery, the VLQ- X can be excluded (at 95% CL limits) in the correlated parameter space of $g^* \in [0.12, 0.4]$ ($[0.06, 0.4]$) and $M_X \in [1000, 1980]$ ($[1000, 2450]$) GeV for the same integrated luminosity. Assuming the non-vanishing R_L value, i.e., $R_L = 0.1$, the discovery region can reach $g^* \in [0.05, 0.39]$ ($[0.025, 0.2]$) and $M_X \in [1000, 3000]$ GeV with an integrated luminosity of 300 (3000) fb^{-1} . Otherwise, the 95% CL excluded region for the coupling parameter g^* is $[0.03, 0.21]$ ($[0.015, 0.11]$) $M_X \in [1000, 3000]$ GeV with the same integrated luminosity at the 14 TeV LHC. Besides, although the vector like quark width plays a significant role in their single production, the region in this study is almost located in $\Gamma_X/M_X < 10\%$, and thus the NWA is reasonable in our study.

The sensitivity that graphicized as contours in $g^* - R_L$ plane is presented in Fig. 7 with $\delta = 10\%$ and five fixed typical $X_{5/3}$ masses at the 14 TeV LHC with an integrated luminosity of 300 and 3000 fb^{-1} , respectively. The current limits from the oblique parameters and the APV experiment are also displayed as dot-dashed curves. One can see that, for $M_X = 1500, 2000, 2500$ GeV and $R_L = 0.1$, the 5σ level discovery sensitivity of g^* is respectively about 0.08, 0.14, 0.24 with an integrated luminosity of 300 fb^{-1} , and changed as about 0.05, 0.14, 0.13 with an integrated luminosity of 3000 fb^{-1} . Otherwise, the 95% CL excluded region for the coupling parameter g^* is respectively about 0.05 (0.025), 0.08 (0.04), 0.14 (0.07)

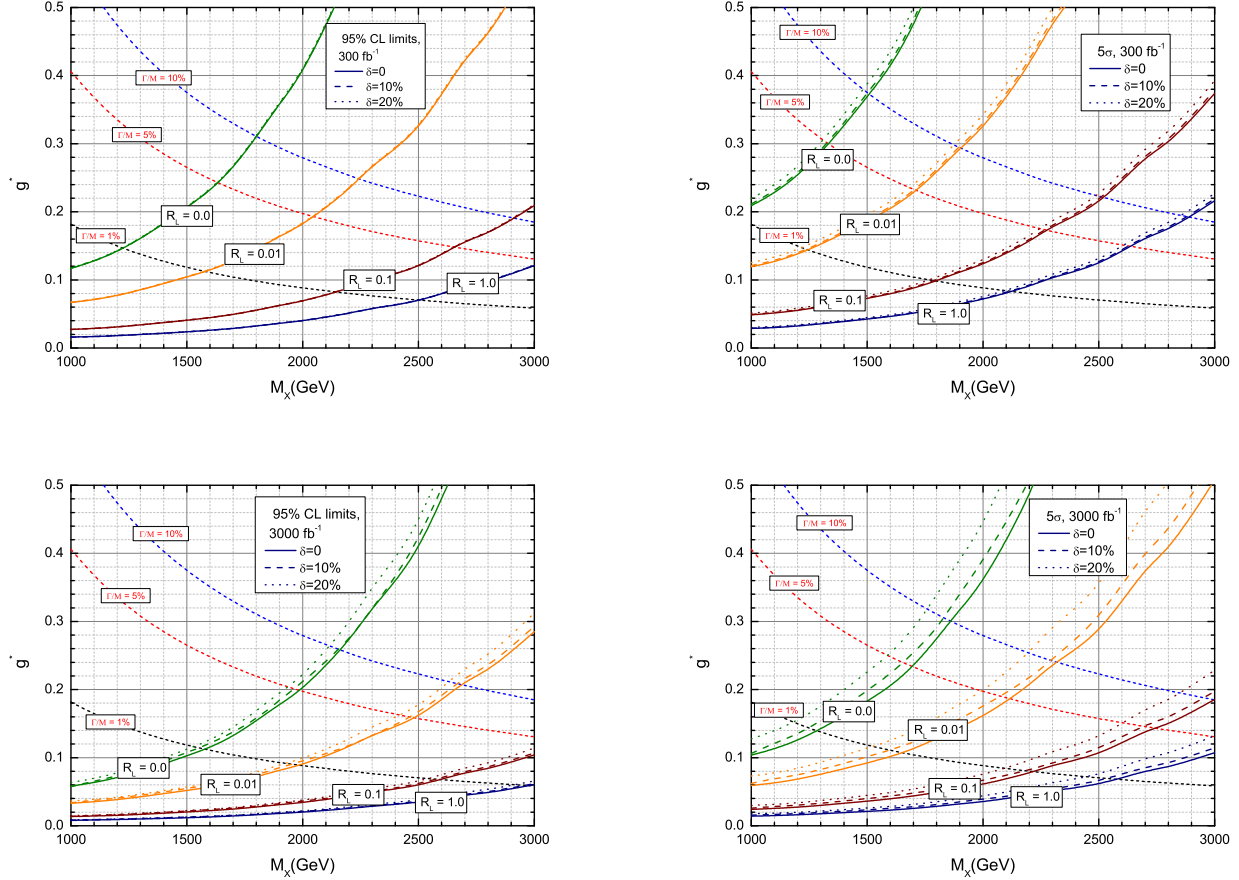


FIG. 6: 95% CL exclusion limit (left panel) and 5σ (right panel) contour plots for the signal in $g^* - M_X$ at the 14 TeV LHC with an integrated luminosity of 3000 fb^{-1} (upper) and 300 fb^{-1} (down). Short-dashed lines denote the contours of Γ_X/M_X .

with an integrated luminosity of 300 (3000) fb^{-1} .

IV. CONCLUSION

We have present a study of the single production of VLQ- X at the future 14 TeV LHC. The work is performed in a simplified model that the SM extended with an SU(2) doublet

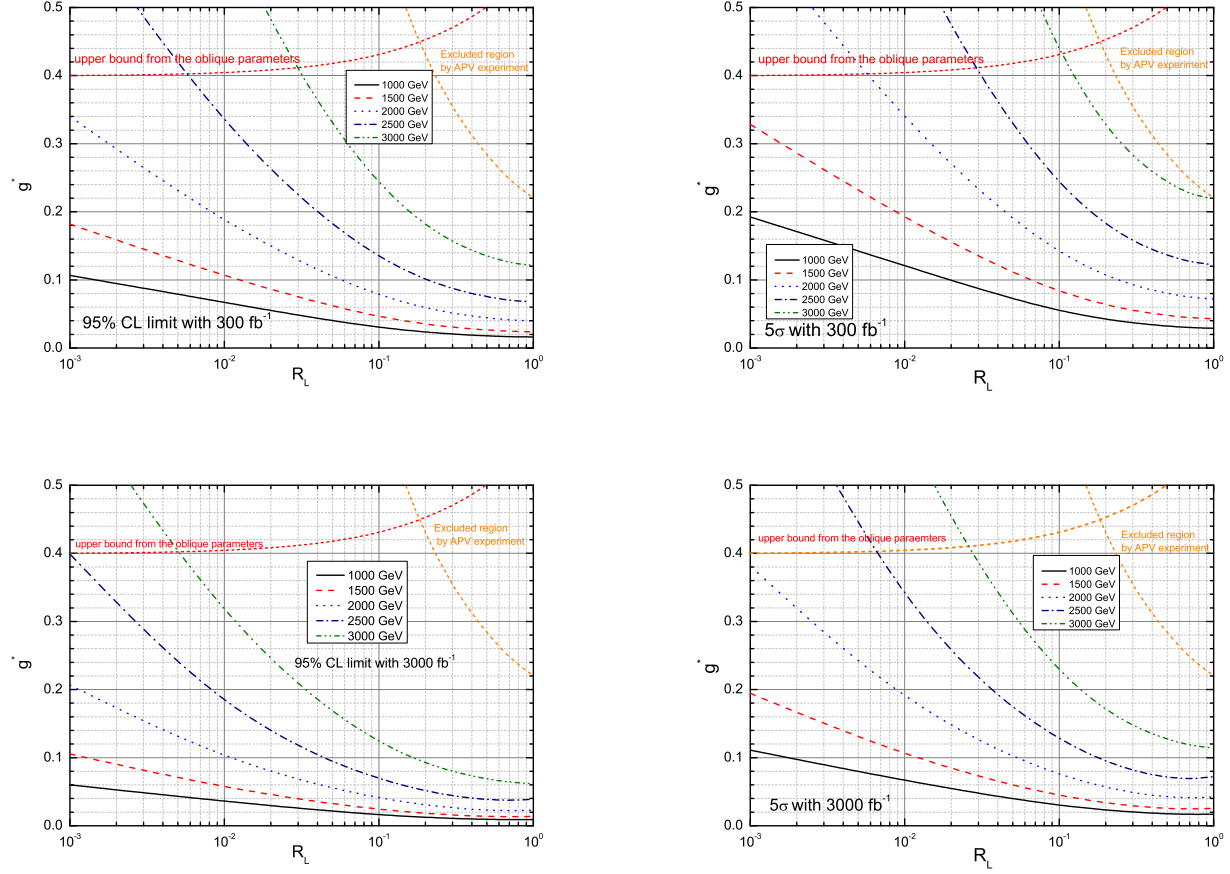


FIG. 7: 95% CL exclusion limit (left panel) and 5σ (right panel) contour plots for the signal in $g^* - R_L$ for five typical mass parameters at 14 TeV LHC with an integrated luminosity of 300 fb^{-1} (upper) and 3000 fb^{-1} (down). Here we take a mild systematic of $\delta=10\%$.

$X_{5/3}$ assuming the VLQ- X coupling only to the first- and preferentially to third-generation quarks. We presented a search strategy at the future HL-LHC for a distinguishable signal with a same-sign dilepton plus one b -tagged jet and missing energy. After performing a detector level simulation for the signal and relevant SM backgrounds, the 5σ discovery prospects and 95% CL exclusion limits in the parameter plane were, respectively, obtained at 14 TeV LHC with an integral luminosity of 300 (3000) fb^{-1} , as displayed in Table III.

Considering a systematic uncertainty of 10%, the LHC run III with an integrated luminosity of 300 fb^{-1} can discover the correlated regions of $g^* \in [0.1, 0.4]$ ($[0.015, 0.22]$) and $M_X \in [1000, 1550]$ $[1000, 3000]$ GeV for $R_L = 0$ (1). On the other hand, the 95% CL exclusion limits are $g^* \in [0.12, 0.4]$ ($[0.01, 0.12]$) and $M_X \in [1000, 1950]$ $[1000, 3000]$ GeV for $R_L = 0$ (1). Meanwhile, the future HL-LHC with an integrated luminosity of 3000 fb^{-1} can discover the correlated regions of $g^* \in [0.1, 0.4]$ ($[0.015, 0.11]$) and $M_X \in [1000, 2000]$ $[1000, 3000]$ GeV for $R_L = 0$ (1). On the other hand, the 95% CL exclusion limits are $g^* \in [0.06, 0.4]$ ($[0.01, 0.06]$) and $M_X \in [1000, 2450]$ $[1000, 3000]$ GeV for $R_L = 0$ (1). This analysis shows that the LHC Run III and future HL-LHC could discover a wide range of parameter space of NP models including VLQ- X . We expect that that our investigation will represent a complementary explorations for a potential $X_{5/3}$ quark at the upgraded LHC.

TABLE III: The 95% CL exclusion limits and 5σ signal discoveries at the LHC Run-III and HL-LHC. The systematic uncertainty is taken as $\delta=10\%$.

R_L	Luminosity (fb^{-1})	Exclusion		Discovery	
		g^*	M_X (GeV)	g^*	M_X (GeV)
0	300	[0.12, 0.4]	[1000, 1950]	[0.21, 0.4]	[1000, 1550]
	3000	[0.06, 0.4]	[1000, 2450]	[0.1, 0.4]	[1000, 2000]
0.01	300	[0.07, 0.4]	[1000, 2650]	[0.12, 0.4]	[1000, 2250]
	3000	[0.034, 0.29]	[1000, 3000]	[0.063, 0.4]	[1000, 2700]
0.1	300	[0.027, 0.21]	[1000, 3000]	[0.05, 0.38]	[1000, 3000]
	3000	[0.014, 0.1]	[1000, 3000]	[0.026, 0.2]	[1000, 3000]
1	300	[0.016, 0.12]	[1000, 3000]	[0.003, 0.22]	[1000, 3000]
	3000	[0.008, 0.06]	[1000, 3000]	[0.015, 0.11]	[1000, 3000]

Acknowledgments

This work is supported by the National Natural Science Foundation of China (Grant No. 11904082)

- [1] L. Susskind, *Phys. Rev. D* **20**, 2619-2625 (1979).
- [2] N. Arkani-Hamed, A. G. Cohen, E. Katz, and A. E. Nelson, *JHEP* **07**, 034 (2002).
- [3] T. Han, H. E. Logan, B. McElrath and L. T. Wang, *Phys. Rev. D* **67**, 095004 (2003).
- [4] S. Chang and H. J. He, *Phys. Lett. B* **586**, 95-105 (2004).
- [5] K. Agashe, R. Contino, and A. Pomarol, *Nucl. Phys. B* **719** 165 (2005).
- [6] P. Lodone, *JHEP* **12**, 029 (2008).
- [7] H. J. He, T. M. P. Tait and C. P. Yuan, *Phys. Rev. D* **62**, 011702(R) (2000).
- [8] X. F. Wang, C. Du and H. J. He, *Phys. Lett. B* **723**, 314-323 (2013).
- [9] H. J. He, C. T. Hill and T. M. P. Tait, *Phys. Rev. D* **65**, 055006 (2002).
- [10] H. J. He and Z. Z. Xianyu, *JCAP* **10**, 019 (2014).
- [11] H. J. He, N. Polonsky and S. f. Su, *Phys. Rev. D* **64**, 053004 (2001).
- [12] N. Chen and H. J. He, *JHEP* **04**, 062 (2012).
- [13] S. Banerjee, M. Frank and S. K. Rai, *Phys. Rev. D* **89**, no.7, 075005 (2014).
- [14] K. Agashe, R. Contino, L. Da Rold and A. Pomarol, *Phys. Lett. B* **641**, 62-66 (2006).
- [15] R. Contino, L. Da Rold and A. Pomarol, *Phys. Rev. D* **75**, 055014 (2007).
- [16] M. Buchkremer, G. Cacciapaglia, A. Deandrea, and L. Panizzi, *Nucl. Phys. B* **876**, 376-417 (2013).
- [17] J. A. Aguilar-Saavedra, R. Benbrik, S. Heinemeyer, and M. Pérez-Victoria,,
Phys. Rev. D **88**, 094010 (2013).
- [18] F. del Aguila, M. Perez-Victoria and J. Santiago, *JHEP* **09**, 011 (2000).
- [19] G. Cacciapaglia, A. Deandrea, N. Gaur, D. Harada, Y. Okada and L. Panizzi, *JHEP* **09**, 012 (2015).
- [20] A. Atre, G. Azuelos, M. Carena, T. Han, E. Ozcan, J. Santiago and G. Unel, *JHEP* **08**, 080 (2011).
- [21] A. De Simone, O. Matsedonskyi, R. Rattazzi and A. Wulzer, *JHEP* **04**, 004 (2013).
- [22] M. Backović, T. Flacke, S. J. Lee and G. Perez, *JHEP* **09**, 022 (2015).
- [23] O. Matsedonskyi, G. Panico and A. Wulzer, *JHEP* **12**, 097 (2014).

- [24] K. P. Xie, G. Cacciapaglia and T. Flacke, [JHEP **10**, 134 \(2019\)](#).
- [25] B. Fuks and H. S. Shao, [Eur. Phys. J. C **77**, no.2, 135 \(2017\)](#).
- [26] J. M. Alves, G. C. Branco, A. L. Cherchiglia, C. C. Nishi, J. T. Penedo, P. M. F. Pereira, M. N. Rebelo and J. I. Silva-Marcos, [Phys. Rept. **1057**, 1-69 \(2024\)](#)
- [27] A. C. Canbay and O. Cakir, [Phys. Rev. D **108**, no.9, 095006 \(2023\)](#)
- [28] M. Aaboud *et al.* [ATLAS], [JHEP **08**, 048 \(2018\)](#).
- [29] M. Aaboud *et al.* [ATLAS], [JHEP **12**, 039 \(2018\)](#).
- [30] M. Aaboud *et al.* (ATLAS Collaboration), [Phys. Rev. Lett. **121**, 211801 \(2018\)](#).
- [31] S. Chatrchyan *et al.* [CMS], [Phys. Rev. Lett. **112**, no.17, 171801 \(2014\)](#).
- [32] A. M. Sirunyan *et al.* [CMS], [JHEP **08**, 073 \(2017\)](#).
- [33] A. M. Sirunyan *et al.* (CMS Collaboration), [Phys. Rev. D **100**, 072001 \(2019\)](#).
- [34] A. Buckley, J. M. Butterworth, L. Corpe, D. Huang, and P. Sun, [SciPost Phys. **9**, 069 \(2020\)](#).
- [35] A. M. Sirunyan *et al.* [CMS], [JHEP **03**, 082 \(2019\)](#).
- [36] G. Aad *et al.* [ATLAS], [Eur. Phys. J. C **83**, no.8, 719 \(2023\)](#).
- [37] S. Moretti, D. O'Brien, L. Panizzi, and H. Prager, [Phys. Rev. D **96**, 075035 \(2017\)](#).
- [38] A. Carvalho, S. Moretti, D. O'Brien, L. Panizzi, and H. Prager, [Phys. Rev. D **98**, 015029 \(2018\)](#).
- [39] A. Deandrea, T. Flacke, B. Fuks, L. Panizzi, and H. S. Shao, [JHEP **08**, 107 \(2021\)](#).
- [40] A. M. Sirunyan *et al.* [CMS], [Eur. Phys. J. C **79**, 90 \(2019\)](#).
- [41] G. Aad *et al.* [ATLAS], [Phys. Rev. D **86**, 012007 \(2012\)](#).
- [42] [ATLAS], [ATLAS-CONF-2012-137](#).
- [43] G. Apollinari, O. Brüning, T. Nakamoto and L. Rossi, [CERN Yellow Rep., 1-19 \(2015\)](#).
- [44] R. Contino and G. Servant, [JHEP **06**, 026 \(2008\)](#).
- [45] G. Cacciapaglia, A. Deandrea, L. Panizzi, S. Perries and V. Sordini, [JHEP **03**, 004 \(2013\)](#).
- [46] J. Ren, R. Q. Xiao, M. Zhou, Y. Fang, H. J. He and W. Yao, [JHEP **06**, 090 \(2018\)](#).
- [47] H. Zhou and N. Liu, [Commun. Theor. Phys. **72**, 105201 \(2020\)](#).
- [48] H. Zhou and N. Liu, [Phys. Rev. D **101**, 115028 \(2020\)](#).
- [49] C. W. Chiang, S. Jana and D. Sengupta, [Phys. Rev. D **105**, no.5, 5 \(2022\)](#).
- [50] F. X. Yang, Z. L. Han and Y. Jin, [Chin. Phys. C **45**, no.7, 073114 \(2021\)](#).
- [51] X. M. Cui, Y. Q. Li and Y. B. Liu, [Phys. Rev. D **106**, no.11, 115025 \(2022\)](#).
- [52] E. Arganda, L. Da Rold, A. Juste, A. D. Medina and R. M. Sandá Seoane, [JHEP **01**, 156 \(2024\)](#).

- [53] S. Chatrchyan *et al.* [CMS], **JHEP** **01**, 154 (2013).
- [54] [ATLAS], **ATLAS-CONF-2012-130**.
- [55] L. Shang and K. Sun, **Nucl. Phys. B** **990**, 116185 (2023).
- [56] J. Z. Han, S. Xu, W. J. Mao and H. Q. Song, **Nucl. Phys. B** **992**, 116235 (2023).
- [57] G. Cacciapaglia, A. Deandrea, L. Panizzi, N. Gaur, D. Harada and Y. Okada, **JHEP** **03**, 070 (2012).
- [58] J. Cao, L. Meng, L. Shang, S. Wang and B. Yang, **Phys. Rev. D** **106**, no.5, 055042 (2022).
- [59] N. Vignaroli, **Phys. Rev. D** **86**, 115011 (2012)
- [60] L. Basso and J. Andrea, **JHEP** **02**, 032 (2015).
- [61] Y. B. Liu, **Phys. Rev. D** **95**, no.3, 035013 (2017).
- [62] G. Cacciapaglia, A. Deandrea, D. Harada and Y. Okada, **JHEP** **11**, 159 (2010).
- [63] J. A. Aguilar-Saavedra, **EPJ Web Conf.** **60**, 16012 (2013).
- [64] D. Vatsyayan and A. Kundu, **Nucl. Phys. B** **960**, 115208 (2020).
- [65] D. Barducci, A. Belyaev, J. Blamey, S. Moretti, L. Panizzi and H. Prager, **JHEP** **07**, 142 (2014).
- [66] J. Alwall, R. Frederix, S. Frixione, V. Hirschi, F. Maltoni, O. Mattelaer, H.-S. Shao, T. Stelzer, P. Torrielli, and M. Zaro, **JHEP** **07**, 079 (2014).
- [67] R. D. Ball *et al.* [NNPDF Collaboration], **JHEP** **04**, 040 (2015).
- [68] B. Jager, C. Oleari and D. Zeppenfeld, **Phys. Rev. D** **80**, 034022 (2009).
- [69] T. Melia, K. Melnikov, R. Rontsch and G. Zanderighi, **JHEP** **12**, 053 (2010).
- [70] J. M. Campbell and R. K. Ellis, **JHEP** **07**, 052 (2012).
- [71] M. Czakon, P. Fiedler and A. Mitov, **Phys. Rev. Lett.** **110**, 252004 (2013).
- [72] T. Sjöstrand, S. Ask, J. R. Christiansen *et al.*, **Comput. Phys. Commun.** **191**, 159 (2015).
- [73] J. de Favereau *et al.* (DELPHES 3 Collaboration), **JHEP** **02**, 057 (2014).
- [74] E. Conte, B. Fuks, and G. Serret, **Comput. Phys. Commun.** **184**, 222 (2013).
- [75] E. Conte, B. Dumont, B. Fuks and C. Wymant, **Eur. Phys. J. C** **74**, no. 10, 3103 (2014).
- [76] G. Cowan, K. Cranmer, E. Gross, and O. Vitells, **Eur. Phys. J. C** **71**, 1554 (2011) [erratum: **Eur. Phys. J. C** **73**, 2501 (2013)].